МРНТИ 27.41.19
УДК 519.6

https://doi.org/10.51889/2022-2.1728-7901.06

STABILIZED FINITE ELEMENT METHOD FOR DETERMINING SATURATION IN THE NON-EQUILIBRIUM FLOW PROBLEM

Baigereyev D.R.[1], Omariyeva D.A.[2], Boranbek K.[2]*

[1] S. Amanzholov East Kazakhstan University, Ust-Kamenogorsk, Kazakhstan
[2] D. Serikbayev East Kazakhstan Technical University, Ust-Kamenogorsk, Kazakhstan
**e-mail: dinara_2205@mail.ru*

Abstract

In this paper, a hybrid finite difference/finite element method for solving the saturation equation in the problem of two-phase non-equilibrium fluid flow in porous media is constructed. The model under consideration is obtained on the basis of the non-equilibrium fluid flow model by S. M. Hassanizadeh with the generalized global pressure concept. Due to the hyperbolic nature of the equation, it has several difficulties leading to the need for a careful choice of the solution method. The classical Galerkin method leads to the appearance of non-physical oscillations at phase interfaces. The paper investigates the application of stabilized finite element methods for their suppression. Three classical stabilized methods are compared: the streamline upwind Petrov-Galerkin (SUPG), the Galerkin least squares (GLS), and the unusual stabilized finite element method (USFEM), and several stabilizing parameters. The comparison of these methods and stabilization parameters is carried out on the basis of three computational experiments.

Keywords: non-equilibrium flows in porous media, stabilized finite element method, SUPG, GLS, USFEM.

Аңдатпа

Д.Р. Байгереев[1], Д.А. Омариева[2], К. Боранбек[2]
[1] С.Аманжолов атындағы Шығыс Қазақстан университеті, Өскемен қ., Қазақстан
[2] Д.Серікбаев атындағы Шығыс Қазақстан техникалық университеті, Өскемен қ., Қазақстан

ЕКІ ФАЗАЛЫ ТЕПЕ-ТЕҢ ЕМЕС АҒЫН ЕСЕБІНДЕГІ ҚАНЫҚТЫҚТЫ АНЫҚТАУДЫҢ ТҰРАҚТАНДЫРЫЛҒАН АҚЫРЛЫ ЭЛЕМЕНТТЕР ӘДІСІ

Бұл жұмыста кеуекті ортадағы сұйықтықтың екі фазалы тепе-тең емес ағымы есебіндегі қанықтық теңдеуін шешуге арналған ақырлы айырымды/ақырлы элементтер гибридті әдісі жасалды. Қарастырылып отырған модель С.М. Хассанизаденің тепе-тең емес сұйықтық ағынының моделі және жалпыланған глобальды қысымы негізінде алынды. Теңдеудің гиперболалық сипатына байланысты, оны шешу бірқатар қиындықтарды туғызады және шешу әдісін мұқият таңдауды қажет етеді. Классикалық Галеркин әдісі фазалардың бөліну шекарасында физикалық емес осцилляциялардың пайда болуына әкеледі. Мақалада оларды жою үшін тұрақтандырылған ақырлы элементтер әдістерін қолдану қарастырылады. Тұрақтандырылған үш классикалық әдіс - Петров-Галеркиннің ағынға қарсы әдісі (SUPG), Галеркиннің ең кіші квадраттар әдісі (GLS) және стандартты емес тұрақтандырылған ақырлы элементтер әдісі (USFEM), сонымен қатар бірнеше тұрақтандырушы параметрлер салыстырылады. Аталған әдістер мен тұрақтандыру параметрлерін салыстыру үшін есептеу тәжірибесі негізінде жүзеге асырылады.

Түйін сөздер: кеуекті ортадағы тепе-тең емес ағындар, тұрақтандырылған ақырлы элементтер әдісі, SUPG, GLS, USFEM.

Аннотация

Д.Р. Байгереев[1], Д.А. Омариева[2], К. Боранбек[2]
[1] Восточно-Казахстанский университет им. С. Аманжолова, Усть-Каменогорск, Казахстан
[2] Восточно-Казахстанский технический университет им. Д. Серикбаева, Усть-Каменогорск, Казахстан

СТАБИЛИЗИРОВАННЫЙ МЕТОД КОНЕЧНЫХ ЭЛЕМЕНТОВ ДЛЯ ОПРЕДЕЛЕНИЯ НАСЫЩЕННОСТИ В ЗАДАЧЕ ДВУХФАЗНОГО НЕРАВНОВЕСНОГО ТЕЧЕНИЯ

В работе построен гибридный метод конечных разностей/конечных элементов для решения уравнения насыщенности в задаче двухфазном неравновесном течении жидкости в пористых средах. Рассматриваемая модель получена на основе модели неравновесного потока жидкости С. М. Хассанизаде с обобщенным глобальным давлением. Из-за гиперболического характера уравнения его решение сопровождается рядом трудностей, приводящих к необходимости тщательного выбора метода решения. Классический метод Галеркина приводит к появлению нефизических осцилляций на границах раздела фаз. В статье исследуется применение стабилизированных методов конечных элементов для их подавления. Сравниваются три классических стабилизированных метода: противопотоковый метод Петрова-Галеркина (SUPG), метод наименьших квадратов Галеркина (GLS) и нестандартный стабилизированный метод конечных элементов (USFEM), а также несколько стабилизирующих параметров. Сравнение этих методов и параметров стабилизации проводится на основе трех вычислительных экспериментов.

Ключевые слова: неравновесные течения в пористых средах, стабилизированный метод конечных элементов, SUPG, GLS, USFEM.

1 Introduction

The dynamics of multiphase fluid flows in porous media depends non-linearly on both the structural and mechanical properties of the fluid and the properties of the surrounding skeleton. However, in real reservoir conditions, the property of delayed phase saturation has a significant influence on the flow process. The study of this behaviour led to the emergence of the theory of non-equilibrium fluid flows in porous media. The need to take this phenomenon into account in the development of oil fields is discussed in many works [1, 2]. It is necessary to take into account non-equilibrium at all stages of oil field development since the dependences of the pressure drop on time obtained during laboratory studies of samples of a porous medium for determining the functions of relative phase permeability differ significantly from the theoretical curves calculated in the framework of the classical theory of fluid flows in porous media. The effect of non-equilibrium can be significant: the time of the saturation establishment in the real oil fields conditions is about a year.

There are several approaches to constructing a non-equilibrium model of fluid flow in porous media. The first approach [3] is based on thermodynamic arguments and volume averaging of microscopic conservation equations of mass and moment. In [3], the concept of dynamic capillary pressure p_c^{dyn}, instantaneous local difference between phase pressures, was introduced, which relates to the static capillary pressure p_c^{stat}, capillary pressure under quasi-static displacement by the relation

$$p_o - p_w = p_c(s) - L\partial_t s,$$

where L is a positive valued phenomenological coefficient and s is the water saturation. During the drainage process, $\partial_t s$ is negative, therefore $p_c^{dyn} > p_c^{stat}$, which is confirmed by experimental observations [4]. Dynamic capillary pressure has been the subject of many experimental [5] and theoretical [6, 7] studies.

The approach proposed by the authors of [3] does not take into account the effects of non-equilibrium on relative phase permeabilities. A more complete model, including the effects of non-equilibrium in both capillary pressure and relative permeability, is proposed by the authors of [8]. An uncountable number of large-scale pore rearrangements occur when the multiphase fluid is displaced. The characteristic time of redistribution for the restructuring of flow networks can be significant. As a result, the flow of each phase does not depend only on the current saturation. The approach under consideration is based on the assumption that instantaneous (dynamic) phase permeabilities and capillary pressure depend on static phase permeabilities and capillary pressure at some effective saturation [9].

In this paper, we consider the non-equilibrium model developed in [3]. First, we construct the computational model by utilizing the generalized global pressure approach. In this case, the equations of the model are reduced to a system of partial differential equations for pressure, velocity and saturation. The saturation equation is of convection-diffusion type with a predominance of convection. The use of the standard Galerkin method leads to the appearance of non-physical oscillations [10, 11]. There are several approaches to suppress these oscillations. One of the approaches is to employ the Galerkin method with discontinuous basis functions, the main disadvantage of which is a significant increase in the number of degrees of freedom. One of the effective ways to construct non-oscillating schemes is to utilize the combined finite element volume method for saturation with the counterflow calculation of the mobility coefficient.

In this work, we use the approach based on the stabilization technique. It consists in adding artificial viscosity to the equation depending on velocity and some stabilizing parameters. The paper deals with the study of the stabilization influence on the sought approximate solution. Specifically, we consider three classical stabilization methods and several stabilizing parameters, and present the numerical tests analysis confirming the effectiveness of their application to the saturation equation in the non-equilibrium flow problem.

2 Formulation of the Problem

Let us consider the problem of two-phase non-equilibrium incompressible fluid flow in porous media with a non-equilibrium law in a bounded convex domain $\Omega \subset R^2$ with a boundary $\Gamma = \Gamma_D \cup \Gamma_N$, $\Gamma_D \cap \Gamma_N = \varnothing$:

$$\phi \partial_t s + \nabla \cdot \vec{u}_w = q_w(p,s), \quad (1)$$

$$-\phi \partial_t s + \nabla \cdot \vec{u}_o = q_o(p,s), \quad (2)$$

$$u_\alpha = -\frac{Kk_\alpha(s)}{\mu_\alpha} \nabla p_\alpha, \alpha \in \{w,o\}, \quad (3)$$

$$p_o - p_w = p_c(s) - L\partial_t s, \quad (4)$$

with initial and boundary conditions

$$s(x,0) = s_o(x), \; x \in \Omega, \quad (5)$$

$$\vec{u}_\alpha \cdot \vec{n} = 0, \; x \in \Gamma, t > 0, \quad (6)$$

where ϕ, K are the porosity and absolute permeability of the medium; the subscript α denotes the phases of water w and oil o, respectively; s is the water saturation; $p_\alpha, k_\alpha, \mu_\alpha, \vec{u}_\alpha$ is the pressure, relative phase permeability, viscosity, and fluid velocity of the phase α, respectively; q_α is the source/sink term; L is substitution time.

We introduce the total velocity vector as follows to obtain a computational model:

$$\vec{u} = \vec{u}_w + \vec{u}_o. \quad (7)$$

By making use of (3) one can easily derive the relation between the total velocity and gradients of phase pressures:

$$\vec{u} = -k(\lambda_w \nabla p_w + \lambda_o \nabla p_o), \quad (8)$$

where $\lambda_\alpha = k_\alpha \mu_\alpha^{-1}$ is the mobility of the phase α. We introduce a new variable, the generalized global pressure p, such that:

$$\lambda_w \nabla p_w + \lambda_o \nabla p_o = \lambda \nabla p, \quad (9)$$

where $\lambda = \lambda_w + \lambda_o$ is the total mobility. By using equations (1)-(4), the explicit form of p can be easily obtained:

$$p = h_w p_w + h_o p_o + \frac{1}{2}(h_w - h_o)p_c - \frac{1}{2}\int_{s_c}^{s} (f_w - f_o) p_c'(\xi) d\xi, \quad (10)$$

where $h_w = h_w(s)$ and $h_o = h_o(s)$ are some functions called weights such that $h_w + h_o = 1$, and $f_\alpha = \frac{\lambda_\alpha}{\lambda}$.

In order to obtain the pressure equation, sum up equations (1) and (2) and use (8) and (9):

$$\begin{aligned} &\nabla \cdot \vec{u} = 0, \\ &(k\lambda)^{-1} \vec{u} + \nabla p = q, \end{aligned} \quad (11)$$

where $q = q_w + q_o$. The phase velocities are expressed in terms of the total velocity by the relation

$$\vec{u}_w = f_w(s)\vec{u} - \gamma(s)\nabla s - \gamma_1(s)\nabla(L\partial_t s), \tag{12}$$

where $\gamma(s) = -K\lambda_o(s) f_w(s)\dfrac{dp_c}{ds} > 0$, $\gamma_1(s) = K\lambda_o(s) f_w(s) > 0$. Substitute (12) into (1) to get the saturation equation:

$$\phi\partial_t s + f_w'(s)\vec{u}\cdot\nabla s - \nabla\cdot(\gamma(s)\nabla s) - \nabla\cdot(\gamma_1(s)\nabla(L\partial_t s)) = q. \tag{13}$$

Thus, the computational model consists of the equations(11), (13) and the corresponding initial and boundary conditions.

In [12], the mixed finite element method was constructed for solving the equations (11), the convergence of the method was investigated and its a posteriori analysis was carried out. In this paper, we focus on solving the equation (13) with the following initial and boundary conditions in more detail:

$$s(x,0) = s_0,\ x \in \overline{\Omega}, \tag{14}$$

$$s = g_D,\ x \in \Gamma_D;\ \nabla s\cdot\vec{n} = g_N,\ x \in \Gamma_N,\ t > 0, \tag{15}$$

Assuming that the vector $\vec{u}$ is known and f, g_D, g_N are given functions. Suppose that this problem has a unique solution in the class of sufficiently smooth functions. For simplicity, we assume that $\phi = 1$.

Let

$$V = \{v \in H^1(0,T;H^1(\Omega)) : v|_{\Gamma_D} = g_D\}, \qquad V_0 = \{v \in H^1(\Omega) : v|_{\Gamma} = 0\}.$$

Next, we define a weak formulation of the problem (13)-(15): find $s \in V$ such that for all $w \in V_0$:

$$(\partial_t s, w) + (\gamma(s)\nabla s, \nabla w) + (f_w'(s)\vec{u}\cdot\nabla s, w) + (\gamma_1(s)\nabla\partial_t s, \nabla w) = (q, w), \tag{16}$$

where $(\cdot,\cdot)$ denotes the scalar product in $L^2(\Omega)$.

Let Ω_h is the quasiuniform partition of Ω and NE is the number of elements in Ω_h. Define the finite element space $V_h \subset V$ as follows:

$$V_h = \{v_h \in H_0^1(\Omega)\cap C^0(\overline{\Omega}) | v_h|_e \in P_1(K)\ \forall K \in \Omega_h\}.$$

Let us introduce a uniform grid on the time interval $[0,T]$ by points $t_n = n\Delta t$, where $\Delta t > 0$ is the time step. Discretize the time derivative in (16) using the backward Euler scheme as follows:

$$\left(\frac{s^n - s^{n-1}}{\Delta t}, w\right) + (\gamma(s^n)\nabla s^n, \nabla w) + (f_w'(s^n)\vec{u}\cdot\nabla s^n, w) + \left(\gamma_1(s^n)\frac{\nabla s^n - \nabla s^{n-1}}{\Delta t}, \nabla w\right) = (q, w). \tag{17}$$

Construct the following iterative method based on (17):

$$\left(\frac{s^{n,m} - s^{n-1}}{\Delta t}, w\right) + (\gamma(s^{n,m-1})\nabla s^{n,m}, \nabla w) + (f_w'(s^{n,m-1})\vec{u}\cdot\nabla s^{n,m}, w) +$$
$$+\left(\gamma_1(s^{n,m-1})\frac{\nabla s^{n,m} - \nabla s^{n-1}}{\Delta t}, \nabla w\right) = (q, w) \tag{18}$$

where $s^{n,m}$ is the sought function at the m-th iteration.

3 Stabilization of the Equation

Let us first consider the special stationary case in which $\gamma_1(s) \equiv 0$, $k_1 = \gamma(s^{n,m-1})$, $\vec{u}_1 = f_w'(s^{n,m-1})\vec{u}$ are known functions. By denoting $s^{n,m} = s$, it follows from (18) that

$$(k_1 \nabla s, \nabla w) + (\vec{u}_1 \cdot \nabla s, w) = (q, w), \ \forall w \in V_0. \tag{19}$$

Seek the solution in the form $s = \sum_{j=1}^{NE} s_j \varphi_j(x)$ where $\varphi_j(x)$ denote the basis functions. According to the standard Galerkin method, we choose $w = \varphi_i(x)$. Thus, we arrive at the following system of equations with respect to s_j:

$$\sum_{j=1}^{NE} \left[(k_1 \nabla \varphi_j, \nabla \varphi_i) + (\vec{u}_1 \cdot \nabla \varphi_j, \varphi_i) \right] s_j = (q, \varphi_i), \ i = \overline{1, NE}.$$

This yields the system of algebraic equations

$$AS = F \tag{20}$$

with elements $A = \lfloor A_{i,j} \rfloor$, $F = [F_i]$,

$$A_{i,j} = (k_1 \nabla \varphi_j, \nabla \varphi_i) + (\vec{u}_1 \cdot \nabla \varphi_j, \varphi_i), \ F_i = (q, \varphi_i), \ S = (s_1, s_2, ..., s_{NE})^{\mathrm{T}}.$$

According to the stabilization technique, we modify the elements of the stiffness matrix $A_{i,j}$ in the following way:

$$A_{i,j}^{stab} = A_{i,j} + \sum_K \tau_K \left(A_{i,j} s_h - q, \tilde{A}_{i,j} \varphi_i \right)_K. \tag{21}$$

The specific choice of the operator $\tilde{A}$ leads to different stabilization methods. For example [13],

$$\begin{aligned} &\text{SUPG}: && \tilde{A} w_h = \vec{u}_1 \cdot \nabla w_h, \\ &\text{GLS}: && \tilde{A} w_h = -\nabla \cdot (k_1 \nabla w_h) + \vec{u}_1 \cdot \nabla w_h, \\ &\text{USFEM}: && \tilde{A} w_h = \nabla \cdot (k_1 \nabla w_h) + \vec{u}_1 \cdot \nabla w_h. \end{aligned} \tag{22}$$

One of the important points in the implementation of stabilized methods is the choice of the stabilization parameter τ_K. The parameter is chosen based on the problem properties, for example, on the principle of discrete maximum, convergence and stability analysis, and others. We give the following examples of the stabilizing parameters for linear elements in accordance with the chosen method [13]:

$$\tau_K^{SUPG} = \begin{cases} \dfrac{h_K}{2|\vec{u}_K|} & \text{when } Pe_K \geq 1, \\[2ex] \dfrac{h_K^2}{12 k_1} & \text{when } Pe_K < 1, \end{cases} \tag{23}$$

$$\tau_K^c = \left(\frac{4k_1}{h_K^2} + \frac{2|\vec{u}_K|}{h_K} \right)^{-1}, \tag{24}$$

$$\tau_K^s = \left(9 \left(\frac{4k_1}{h_K^2} \right)^2 + \left(\frac{2|\vec{u}_K|}{h_K} \right)^2 \right)^{-\frac{1}{2}}, \tag{25}$$

$$\tau_K^a = \left(\frac{12k_1}{h_K^2} + \frac{2|\vec{u}_K|}{h_K^2} \right)^{-1}, \tag{26}$$

$$\tau_K^{fv} = \left(\frac{6k_1}{h_K^2} \zeta\left(\frac{|\vec{u}_K| h_K}{3k_1} \right) \right)^{-1}, \tag{27}$$

where $Pe_K = \frac{|\vec{u}_k| h_K}{6k_1}$, h_K is diameter of the triangle K.

In the non-stationary case, the matrix A and the vector F depend on time. Let A_n and F_n denote the matrix A and vector F evaluated at $t = t_n$. Then (18) reduces to the system of algebraic equations

$$S_n = \left(M + \Delta t A_n^{stab}\right)^{-1}\left(MS_{n-1} + \Delta t F_n\right),$$

where M is the mass matrix, S is the solution of (16) at $t = t_n$.

4 Comparison of the Stabilizing Parameters

Let us compare the stabilization methods (22) and the stabilizing parameters (23)-(27) based on three computational experiments. The first computational experiment is to test the stabilization effect on the approximate solution using the SUPG method as an example. The second computational experiment is to estimate the deviation from the upper and lower bounds of the solution using stabilization methods and stabilizing parameters and different grid configurations. The third computational experiment is to compare an approximate solution with a known exact solution.

Example 1. In $\Omega = [0,1]^2$, consider the problem (15), (19) with the parameters $\vec{u}_1 = \left(\sqrt{2}/2, -\sqrt{2}/2\right)$, $k_1(x) \equiv 10^{-4}$, $q = 0$, $\Gamma_N = \varnothing$, and

$$g_D(x) = \begin{cases} 1, & x \in \{(x_1, x_2): x_1 = 0, x_2 \le 0.8 \text{ or } x_2 = 0, x_1 \le 0.8\}, \\ 0, & \text{otherwise}. \end{cases}$$

Choosing the coefficient k_1 in this form makes the problem with a predominance of convection. This equation has a gap along the straight line $x_2 = -0.8 + x_1$, including at the point $(0, 0.8)$ on the boundary of the domain. Figure 1 (a) and Figure 1 (b) shows the solution obtained without stabilization on different meshes with different level of thickness. During computational experiments, thickening the grid along the gap line and near the break at the border does not fully suppress the oscillations. Figure 1 (c) shows that the stabilization significantly improves the quality characteristics of the approximate solution.

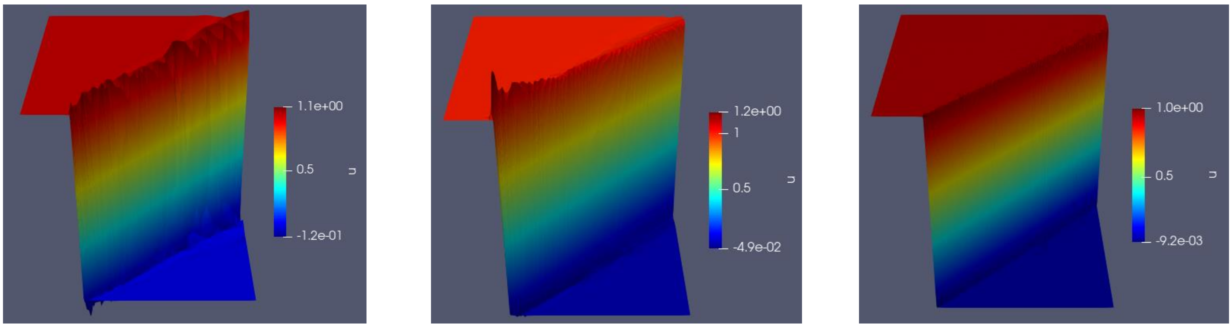

a) b) c)

Figure 1. Thickening the grid and using the stabilized method
a) Thickening the grid near a break at the boundary; b) Thickening the grid along the gap line;
c) The use of the stabilized method.

Example 2. Let $Q_T = \Omega \times (0,T)$, where Ω is a unit square as in Example 1, and $\Gamma_D = \Gamma_{D_0} \cup \Gamma_{D_1}$, $\Gamma_{D_0} = \{x \in \Gamma : x_2 = 0\}$, $\Gamma_{D_1} = \{x \in \Gamma : x_1 = 0 \text{ or } x_1 = 1\}$, and $\Gamma_N = \Gamma \setminus \Gamma_D$. In Q_T, consider the equation (13) with the parameters $T = 1$, $\vec{u} = (0.15, 1)$, $\gamma(s) \equiv 10^{-4}$, $\gamma_1(s) \equiv 0$, $f_w(s) = s$, and the initial and boundary conditions are as follows:

$s(x,0) = 0,\ g_D(x) = \begin{cases} 1, & x \in \Gamma_{D_1}, \\ 0, & x \in \Gamma_{D_0}, \end{cases}\ g_N(x) = 0.$ In the computational experiment, three grid configurations were used, which contain 968, 3744 and 15110 elements. The value of the parameter τ is set to 10^{-2}. The calculations were performed until the time layer $n = 100$ was achieved, which corresponds to the time value $T = 1$. Obviously, the values of the exact solution are between 0.00 and 1.00. Implementation of (22) without the use of stabilization leads to the appearance of non-physical oscillations the absolute value of which is more than 60% (Table 1).

Table 1. Boundaries of the interval containing the values of the exact and approximate solutions

NE	*Exact bounds*		*Without stabilization*		*SUPG+ τ_c*		*GLS+ τ_c*		*USFEM+ τ_c*	
	lower	*upper*	*lower*	*upper*	*lower*	*upper*	*lower*	*upper*	*lower*	*upper*
968	*0.00*	*1.00*	*-0.38*	*1.74*	*-0.04*	*1.04*	*-0.03*	*1.03*	*-0.04*	*1.03*
3774	*0.00*	*1.00*	*-0.30*	*1.32*	*-0.03*	*1.02*	*-0.02*	*1.01*	*-0.03*	*1.01*
15110	*0.00*	*1.00*	*-0.21*	*1.17*	*-0.02*	*1.00*	*-0.02*	*1.01*	*0.01*	*1.01*

The upper row of Figure 2 shows an approximate solution without the use of stabilization at $t = t_{10}$, t_{50}, t_{100}, and in the lower row with the use of the SUPG method and the stabilization parameter τ_c. Table 1 illustrates the deviation dependence of the approximate solution on the exact bounds, depending on the choice of the stabilization method and the stabilizing parameters. Stabilization made it possible to reduce the deviation from the exact boundaries to less than 3% for all of the three methods considered.

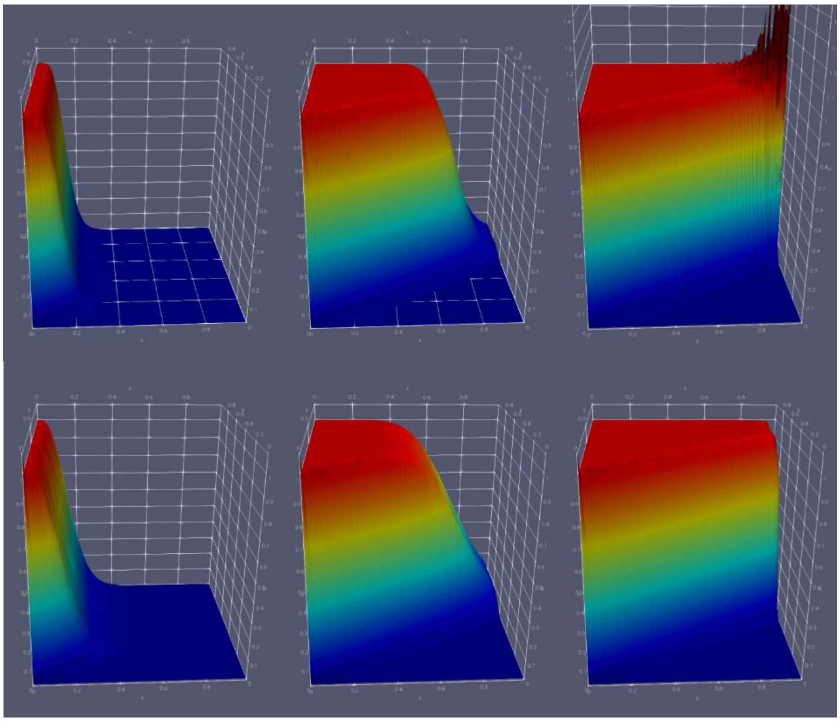

Figure 2. The approximate solution of the Example 2.

Example 3. In $Q_T = \Omega \times (0,T)$, where $\Omega = (-0.5,0.5) \times (-0.5,0.5)$ the problem (15), (19) with the parameters $\gamma(s) \equiv k_1 = 10^{-4}$, $\vec{u} = \left(1/\sqrt{2}, 1/\sqrt{2}\right)$, $f_w(s) = s$, and the right-hand side

$$f(x,t) = -\frac{1}{\sqrt{2}\varepsilon}\phi^2(x,t,\varepsilon) + \frac{1}{2\varepsilon}\phi^2(x,t,\varepsilon) - \frac{1}{\varepsilon^2}k_1\phi^2(x,t,\varepsilon)\tanh\left(\frac{x_1+x_2-t}{2\varepsilon}\right) - $$
$$-k_2\left[\frac{1}{\varepsilon^3}\phi^2(x,t,\varepsilon)\tanh\left(\frac{x_1+x_2-t}{2\varepsilon}\right)^2 - \frac{1}{2\varepsilon^3}\phi^4(x,t,\varepsilon)\right]$$

is considered where $\phi(x,t,\varepsilon) = \mathrm{sech}((x_1+x_2-t)/2\varepsilon)$, $\gamma_1(s) \equiv k_2 = \mathrm{const}$, and $\varepsilon = 10^{-2}$. The exact solution of the problem is $s(x,t) = 0.5 - \tanh((x_1+x_2-t)/2\varepsilon)$.

In this computational experiment, the accuracy value was estimated in the L^2-norm. Two values of the parameter τ equal to 1/30 and 1/60 are accepted. The grid configuration was chosen in the same way as in Example 2. To estimate the influence of the term with the third derivative of the solution, we considered two cases, $k_2 = 10^{-6}$ and $k_2 = 10^{-2}$. According to the results of numerical tests presented in Tables 2 and 3, SUPG was the most effective in the first case, and GLS and USFEM were in the second case.

Table 2. L^2-errors of the approximate solution depending on the stabilization method and stabilizing parameters when $k_2 = 10^{-6}$

Methods	N_e	$\tau = 1/30$				$\tau = 1/60$			
		τ_K^c	τ_K^s	τ_K^a	τ_K^f	τ_K^c	τ_K^s	τ_K^a	τ_K^f
Without stabilization	*968*	*1.3052*	*1.2246*	*1.1218*	*1.1089*	*1.1473*	*1.0045*	*0.8286*	*1.0083*
	3744	*0.9934*	*0.9924*	*0.8214*	*1.0086*	*0.9645*	*0.8531*	*0.5425*	*0.8028*
	15110	*0.7911*	*0.8512*	*0.7457*	*0.7645*	*0.7654*	*0.7491*	*0.4289*	*0.6732*
SUPG	*968*	*0.0615*	*0.0717*	*0.0754*	*0.0718*	*0.0243*	*0.0283*	*0.0192*	*0.0185*
	3744	*0.0312*	*0.0499*	*0.0447*	*0.0413*	*0.0171*	*0.0089*	*0.0093*	*0.0090*
	15110	*0.0091*	*0.0248*	*0.0098*	*0.0200*	*0.0033*	*0.0045*	*0.0047*	*0.0043*
GLS	*968*	*0.0723*	*0.0792*	*0.0749*	*0.0721*	*0.0247*	*0.0285*	*0.0288*	*0.0287*
	3744	*0.0425*	*0.0447*	*0.0432*	*0.0496*	*0.0179*	*0.0089*	*0.0090*	*0.0093*
	15110	*0.0212*	*0.0219*	*0.0213*	*0.0236*	*0.0132*	*0.0041*	*0.0043*	*0.0041*
USFEM	*968*	*0.0547*	*0.0545*	*0.0557*	*0.0589*	*0.0076*	*0.0189*	*0.0191*	*0.0190*
	3744	*0.0346*	*0.0475*	*0.0345*	*0.0315*	*0.0527*	*0.0095*	*0.0096*	*0.0095*
	15110	*0.0129*	*0.0212*	*0.0237*	*0.0132*	*0.0497*	*0.0043*	*0.0042*	*0.0044*

Table 3. L^2-errors of the approximate solution depending on the stabilization method and stabilizing parameters when $k_2 = 10^{-2}$

Methods	N_e	$\tau = 1/30$				$\tau = 1/60$			
		τ_K^c	τ_K^s	τ_K^a	τ_K^f	τ_K^c	τ_K^s	τ_K^a	τ_K^f
Without stabilization	*968*	*1.2211*	*1.1835*	*1.0256*	*1.1164*	*1.2858*	*1.1764*	*1.2014*	*1.3875*
	3744	*0.6547*	*0.7436*	*0.9182*	*0.8384*	*1.0645*	*0.7621*	*0.8574*	*1.0064*
	15110	*0.4583*	*0.5487*	*0.6365*	*0.5912*	*0.6257*	*0.4471*	*0.6314*	*0.5947*
SUPG	*968*	*0.0689*	*0.0708*	*0.0658*	*0.0618*	*0.0296*	*0.0187*	*0.0214*	*0.0173*
	3744	*0.0252*	*0.0338*	*0.0228*	*0.0294*	*0.0131*	*0.0114*	*0.0112*	*0.0117*
	15110	*0.0128*	*0.0100*	*0.0111*	*0.0182*	*0.0068*	*0.0051*	*0.0054*	*0.0058*
GLS	*968*	*0.0558*	*0.0587*	*0.0587*	*0.0554*	*0.0141*	*0.0114*	*0.0047*	*0.0146*
	3744	*0.0268*	*0.0241*	*0.0248*	*0.0223*	*0.0054*	*0.0047*	*0.0075*	*0.0052*
	15110	*0.0193*	*0.0187*	*0.0158*	*0.0187*	*0.0021*	*0.0024*	*0.0036*	*0.0027*
USFEM	*968*	*0.0518*	*0.0514*	*0.0525*	*0.0582*	*0.0647*	*0.0141*	*0.0116*	*0.0112*
	3744	*0.0284*	*0.0251*	*0.0287*	*0.0237*	*0.0574*	*0.0051*	*0.0057*	*0.0053*
	15110	*0.0161*	*0.0163*	*0.0178*	*0.0187*	*0.0331*	*0.0029*	*0.0025*	*0.0021*

5 Conclusion

Based on the results of the conducted studies, it can be concluded that the use of stabilization has significantly improved the qualitative pattern of the sought approximate solution. The presented numerical examples illustrate the effectiveness of the proposed approach to solving the saturation equation in the problem of two-phase non-equilibrium fluid flow problem.

In future works, the authors intend to strictly theoretically study the stability and convergence of the proposed numerical schemes. In addition, a separate work will be devoted to the study of the non-equilibrium effects within the framework of the considered model using more realistic data.

6 Acknowledgements

The work was supported by grant funding of Ministry of Education and Science of the Republic of Kazakhstan, grant No. AP08053189, 2020-2022.

References:

1 Amaziane B., Panfilov M., Pankratov L. (2016) Homogenized Model of Two-Phase Flow with Local Nonequilibrium in Double Porosity Media // Advances in Mathematical Physics, Vol. 2016 (3058710), 1-14. https://doi.org/10.1155/2016/3058710

2 Sukharev M. (2020) Fluid Mixing Nonequilibrium Processes in Industrial Piping Flows // Energy, Vol. 13 (6364), 1-18. https://doi.org/10.3390/en13236364

3 Hassanizadeh S.M. (2015) Handbook of Porous Media (edited by Kambiz Vafai). Florida, US: CRC Press, Chapter 2, 47-62.

4 Hassanizadeh S.M., Celia M.A., Dahle H.K. (2002) Dynamic Effects in the Capillary Pressure-Saturation Relationship and Its Impact on Unsaturated Flow // Vadose Zone Journal, Vol. 1 (1), 38–57. http://dx.doi.org/10.24200/jams.vol7iss2pp69-71

5 Zhuang L, Hassanizadeh S., Qin C, Wall A. (2017) Experimental Investigation of Hysteretic Dynamic Capillarity Effect in Unsaturated Flow // Water Resources Research, Vol. 53, 9078-9088 https://doi.org/10.1002/2017WR020895

6 Goel G., Abidoye L. K., Chahar B. R., Das D. B. (2016) Scale dependency of dynamic relative permeability saturation curves in relation with fluid viscosity and dynamic capillary pressure effect // Environmental Fluid Mechanics, Vol. 16, 945–963. https://doi.org/ 10.1007/s10652-016-9459-y

7 Tang M., Zhan H., Ma H., Lu S. (2018) Upscaling of Dynamic Capillary Pressure of Two-Phase Flow in Sandstone // Water Resources Research, Vol. 55 (1), 426-443. https://doi.org/10.1029/2017WR022377

8 Barenblatt G.I., Patzek T. W., Silin D. B. (2003) The Mathematical Model of Nonequilibrium Effects in Water-Oil Displacement // SPE Journal., Vol. 8 (4), 409-416. https://doi.org/10.2118/87329-PA

9 Juanes R. (2008) Non-equilibrium Effects in Models of Three-Phase Flow in Porous Media. // Advances in Water Resources., Vol. 31 (4), 661–673. http://dx.doi.org/10.1016/j.advwatres.2007.12.005

10 Ladubec C., Gracie R. (2016) Stabilized Finite Element Methods for Vertically Averaged Multiphase Flow for Carbon Sequestration // International Journal for Numerical Methods in Engineering, Vol. 111 (8), 724-752. https://doi.org/10.1002/nme.5480

11 Roggendorf S. (2019) Eliminating the Gibbs Phenomenon: The Non-linear Petrov-Galerkin Method for the Convection-diffusion-reaction Equation. Nottingham, UK: University of Nottingham. http://eprints.nottingham.ac.uk/59436/

12 Baigereyev D. R., Temirbekov N. M., Omarieva D. A. (2020) Construction of an iterative method for solving nonlinear equation of elliptic type on the basis of the mixed finite element method. // Bulletin of KazNU. Series mathematics, mechanics, computer science., Vol. 106 (2), 104–120. https://doi.org/10.26577/JMMCS.2020.v106.i2.09.

13 Sendur A. (2018) A Comparative Study on Stabilized Finite Element Methods for the Convection-Diffusion-Reaction Problems // Journal of Applied Mathematics, Vol. 2018, 4259634, 1-17. https://doi.org/10.1155/2018/4259634